ICARUS 47, 184–202 (1981)

Stratigraphy of the Caloris Basin, Mercury

JOHN F. MCCAULEY

U.S. Geological Survey, Flagstaff, Arizona 86001

JOHN E. GUEST

University of London Observatory, London, United Kingdom

GERALD G. SCHABER

U.S. Geological Survey, Flagstaff, Arizona 86001

NEWELL J. TRASK

U.S. Geological Survey, Reston, Virginia 22092

AND

RONALD GREELEY

Arizona State University, Tempe, Arizona 85281

Received May 5, 1980; revised July 1, 1981

The 1300-km-diameter Caloris impact basin is surrounded by well-defined ejecta units that can be recognized from more than 1000 km, radially outward from the basin edge. A formal rock stratigraphic nomenclature is proposed for the Caloris ejecta units, which are collectively called the *Caloris Group*. Each of the individual formations within the Group are described and compared to similar rock units associated with the lunar Imbrium and Orientale basins. A crater degradation chronology, linked the the Caloris event, is also proposed to assist in stratigraphic correlation on a Mercury-wide basis.

INTRODUCTION

The Caloris basin is surrounded by an extensive ejecta blanket that has been described by Trask and Guest (1975), Strom *et al.* (1975), McCauley (1977), and Guest and O'Donnell (1977). The Caloris basin and its associated ejecta dominate much (about 20%) of the outgoing Mariner 10 mosaic of Mercury. Almost half of the basin is visible; its pictorial setting is very similar to that of the Orientale basin in the Lunar Orbiter IV photographs. The Caloris basin is surrounded by a belt of blocky terrain 1 to 2 km high (estimated from shadow lengths) and 100 to 150 km wide called Caloris Montes. The inner diameter of this encompassing ring structure is about 1300 km. A discontinuous, weakly expressed scarp surrounds the blocky terrain beyond which lineated terrain, first identified as Caloris ejecta by Trask and Guest (1975), extends as far as the large crater Shakespeare, 1000 km northeast of the inner edge of Caloris Montes. The Caloris ejecta is covered around much of the basin by an enormous annulus of non lineated smooth plains material that extends outward from Caloris Montes more than 1400 km.

As on the Moon, where ejecta from the better-preserved impact basins such as Imbrium (Shoemaker and Hackman, 1962), Orientale (McCauley, 1967), and Nectaris

0019-1035/81/080184-19$02.00/0

(Stuart-Alexander and Wilhelms, 1975) were used to establish a regional stratigraphy, the ejecta from Caloris also can be used as a marker horizon. We here propose a formal rock-stratigraphic nomenclature for the distinctive deposits that encompass the Caloris basin and are clearly related to it. This nomenclature was developed during 1:5,000,000-scale geologic mapping of the Tolstoj (H-8) (Schaber and McCauley, 1980) and adjacent Shakespeare (H-3) (Guest and Greeley, 1981) quadrangles, and is a refinement of the earlier photogeologic work of the Mariner 10 Experiment Team. The stratigraphy described is patterned, with some modification, after that used in geologic mapping of the Imbrium basin by Wilhelms and McCauley (1971) and the Orientale basin by Scott *et al.* (1977). Certain morphologically similar assemblages of materials around Caloris are recognized which have mappable distribution patterns and can be treated as discrete rock-stratigraphic units. Figure 1 summarizes the current stratigraphic nomenclature for Orientale, Imbrium, and the nomenclature proposed for Caloris. Morphologically similar units around each of the basins are aligned vertically.

Unlike the original lunar stratigraphy of Shoemaker and Hackman (1962), that given here is rock-stratigraphic rather than time-stratigraphic, i.e., no systems and accompanying periods of time such as the Imbrian, Eratosthenian, and Copernican are defined. A time-stratigraphy for the more geologically complex surface of Mars has been developed by Scott and Carr (1979) in

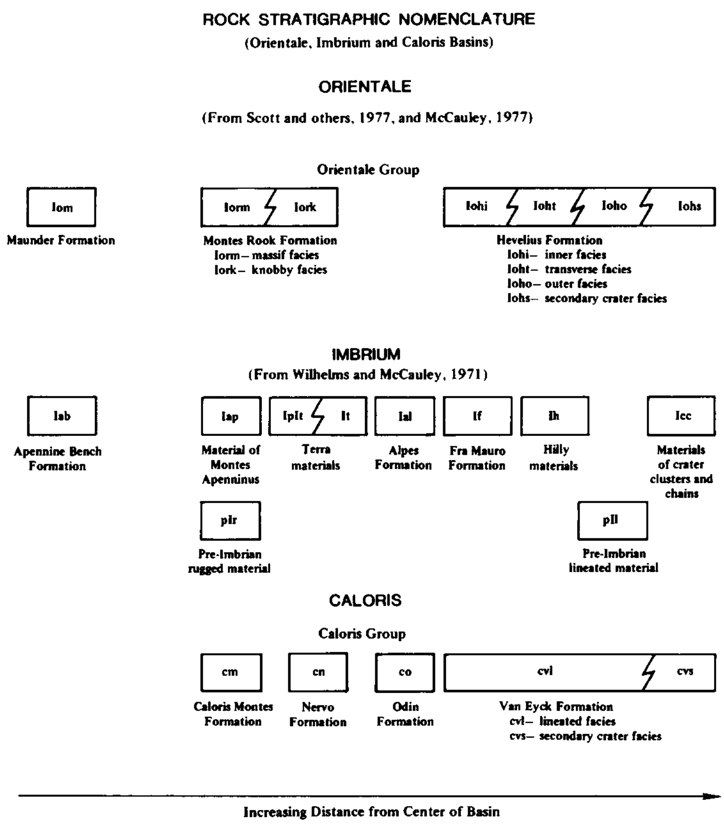

FIG. 1. Summary of rock stratigraphy for Orientale and Imbrium and that proposed here for Caloris. Morphologically similar units around each basin are in approximate vertical alignment. Horizontal alignment reflects approximate relative distance of each unit from the inferred center of the basin.

a planetwide synthesis of the earlier 1:5,000,000-scale geologic mapping program. A formal time-stratigraphy for Mercury would be premature at this time because of the limited Mariner 10 data.

The geologic history of Mercury has been discussed by various investigators including Davies *et al.* (1978) and Strom (1978). Five epochs in the geologic history of Mercury are generally recognized ranging from the condensation of the solar nebula, through the culmination of the period of heavy meteorite bombardment, the Caloris event, a time of plains formation, and finally to the long period of relative inactivity and scattered crater formation that reaches to the present. These sequences of geologic events do not represent a formal time-stratigraphy because they are not tied to actual rock sequences.

We here propose the establishment of a single rock-stratigraphic group consisting of a number of individual Caloris-related formations. According to stratigraphic practice, groups are recognized for the purpose of expressing the natural relations between associated formations, and the group consists of divisions that are formally named formations (Cohee, 1974, pp. 4,8). The formation is, however, the fundamental unit in rock-stratigraphic classification, and mappability is essential to its validity. We intend here to formally define four laterally gradational but mappable formations on Mercury that are synchronous with the Caloris basin. These impact-produced units are morphologically and also probably lithologically, distinct from one another and are akin to the various basin-related rock-stratigraphic units recognized on the Moon.

LUNAR COMPARISONS AND GENERAL CONSIDERATIONS

Although it is the youngest and largest of the Mercurian basins seen so far, Caloris is more degraded than the two youngest basins on the Moon, Orientale and Imbrium. Caloris does, however, have much in common with these lunar basins. Similarities between Orientale and Caloris have been pointed out by Strom *et al.* (1975) and by McCauley (1977).

McCauley (1977) described the morphologic dissimilarities between the four rings of Orientale and emphasized their general lack of circumferential continuity. Much attention has been given to the ring structures in and around lunar basins, and there are many widely divergent opinions as to how these features developed during the cratering process (Head, 1974; Moore *et al.*, 1974; Hodges and Wilhelms, 1976; Wilhelms *et al.*, 1977). Differences in the nature of the target material, the projectile itself, the angle and speed of impact, and the gravitational field are some of the variables that affect the size and shape of the final crater and the distribution of ejecta and secondary craters. Regardless of these complexities, impact cratering is an orderly process with characteristic types of deposits and structures formed in and around the final cavity of excavation (Shoemaker, 1962, 1963; Gault *et al.*, 1968; Oberbeck, 1975; Morrison and Oberbeck, 1975; Gault *et al.*, 1975; Roddy, 1976).

On the basis of morphology, McCauley (1977) showed that the materials that make up the Montes Rook at Orientale are similar to those of the Caloris Montes. Both arcuate mountain ranges consist of jumbled, roughly rectilinear blocks or massifs mostly about 10 to 50 km long and several kilometers high that form a distinct belt around the inner and lower parts of each basin. The Caloris Montes vary somewhat in morphology circumferentially around the basin, but they are different from the terrain farther from the edge of the basin. A similar situation prevails in the Montes Rook around Orientale where the mountains on the north and south sides of the basin are less blocky and have stronger radial trends than elsewhere (Fig. 2). Over much of the extent of the Montes Rook, the long axes of the blocks are either radial to, or concentric with, the center of the basin, but locally

FIG. 2. The Orientale basin. The small arrows point to the massif facies of the Montes Rook Formation. The easternmost small arrow points to a probable tear fault in Montes Rook. The broad upward-curving arrows point to the knobby facies of the Montes Rook Formation, the northernmost large arrow indicates where the discontinuous Cordillera scarp is overlain by knobby facies. Larger patches of knobby facies lie outside the Cordillera scarp on the southwest side of the basin (not visible in this photograph). The downward-curving broad arrow shows typical swirly material on the inner facies of the Hevelius Formation. The outer facies of the Hevelius does not show well in this picture (Lunar Orbiter IV-M187).

they are sharply askew from both these directions and appear to be imbricated with one another. The broad arc of blocky to knobby deposits that forms the Montes Rook is also interrupted by numerous vague depressions and radially oriented graben-like troughs.

The materials surrounding the inner parts of Orientale form a distinctive annulus 100 to 150 km wide that has been designated as the Montes Rook Formation by Scott *et al.* (1977) and McCauley (1977). The blocky materials discussed above—the massif facies of the Montes Rook—are interpreted as intensely deformed parts of the original crater rim probably covered with late-arriving fallback. The large blocks grade into smaller knobs set in a matrix of smooth rolling plains. These knobs and plains make up a unit, called the knobby facies of the Montes Rook Formation, which probably consists of coherent chunks of material from deep within the basin surrounded by more finely crushed ejecta.

The Montes Rook Formation differs markedly from the materials farther from the center of the basin. These more distal materials form an even broader annulus or blanket around Orientale that is hundreds to more than 1000 kilometers wide. These materials have been called the Hevelius Formation and were divided into an inner and outer facies (Scott *et al.*, 1977). The inner facies is most readily recognized near the edge of or just beyond the Montes Cordillera scarp, but its contacts with the Montes Rook Formation are irregular, and large lobes of the knobby facies of the latter formation lie well beyond the Cordillera scarp to the north and southwest of the basin. The inner facies of the Hevelius Formation is characterized by numerous closely spaced, smooth-appearing, elongate depressions separated by wavy to locally swirly ridges. Some concentric ridge structure is present on the east side of Orientale where the unit is thinner than elsewhere and does not completely obscure the rims of the larger prebasin craters. The dominant trend or grain of this unit, however, is radial to the basin center.

The inner facies of the Hevelius Formation is considered a continuous groundcover that was emplaced at low angles and with considerable radial momentum. Secondary cratering is an important mechanism of emplacement according to Morrison and Oberbeck (1975). Their model envisioned a dense rain of projectiles thrown from the expanding basin cavity early in its development. This produced an outward-moving, ground-hugging surge of material that mixed extensively with the prebasin bedrock. With increasing distance from the basin, the secondaries and their ejecta are more widely dispersed, and the basin-related ground cover become thin to discontinuous. The outer facies of the Hevelius is less swirly than the inner facies, only partly obscures prebasin terrain, and is more strongly lineated in the radial direction. It apparently consists of a greater proportion of secondary crater material than does the inner facies. The boundary between the inner and outer facies is readily mappable as demonstrated by Scott *et al.* (1977), but the boundary between the outer facies and the rest of the Moon is highly dependent on the resolution of available photographs and is generally difficult to map.

Although similar in many respects to Orientale, the Caloris basin seems to have even more in common with the Imbrium basin (Fig. 3). The arcuate mountains that surround the central basin of Imbrium (Montes Carpatus, Apenninus, Caucasus and Alpes) are morphologically similar to Montes Caloris. Large blocks or massifs forming a highly segmented and discontinuous mountain belt that encompasses a central circular low are present at both Caloris and Imbrium. Circumferential trends as well as weakly to moderately well developed radial trends are present at different places around each basin, but regardless of the type of trend, massifs dominate the topography. Around Imbrium,

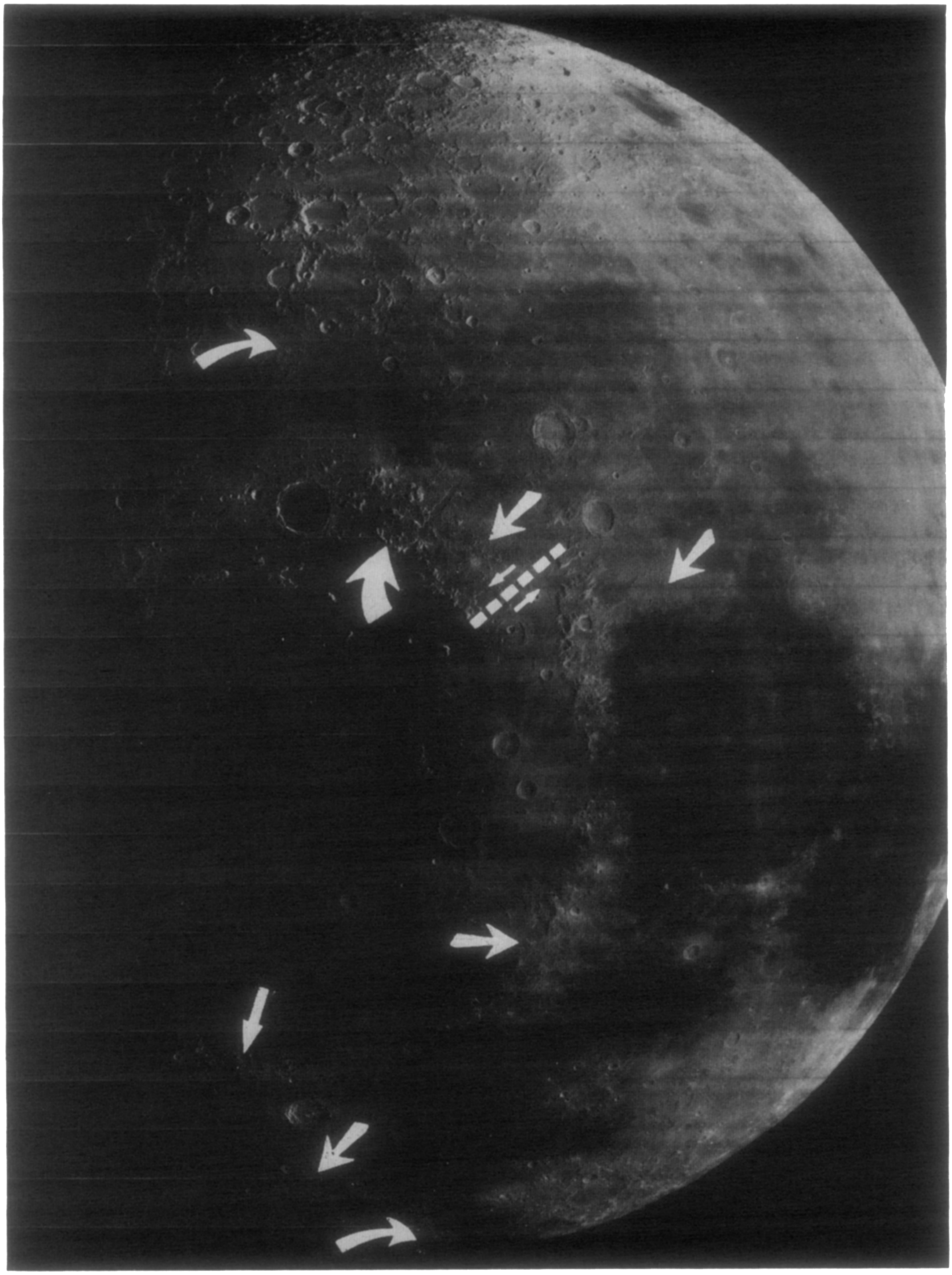

FIG. 3. The Imbrium basin. The broad upward-curving arrow shows Montes Alpes, the narrow southward-pointing arrow Montes Carpatus, and the small east-pointing arrow Montes Apenninus. Although there are minor circumferential variations in texture, these basin encompassing mountains are morphologically more similar to the massif facies of the Montes Rook Formation than to other basin-related units. The three small southwest-pointing arrows indicate typical occurrences of the Alpes Formation lying beyond the Imbrium rim. The eastward-curving arrows on the north and south show typical Fra Mauro Formation. The inferred tear fault that disrupts the continuity of the Imbrium rim is shown by a heavy dashed line (Lunar Orbiter IV-M115).

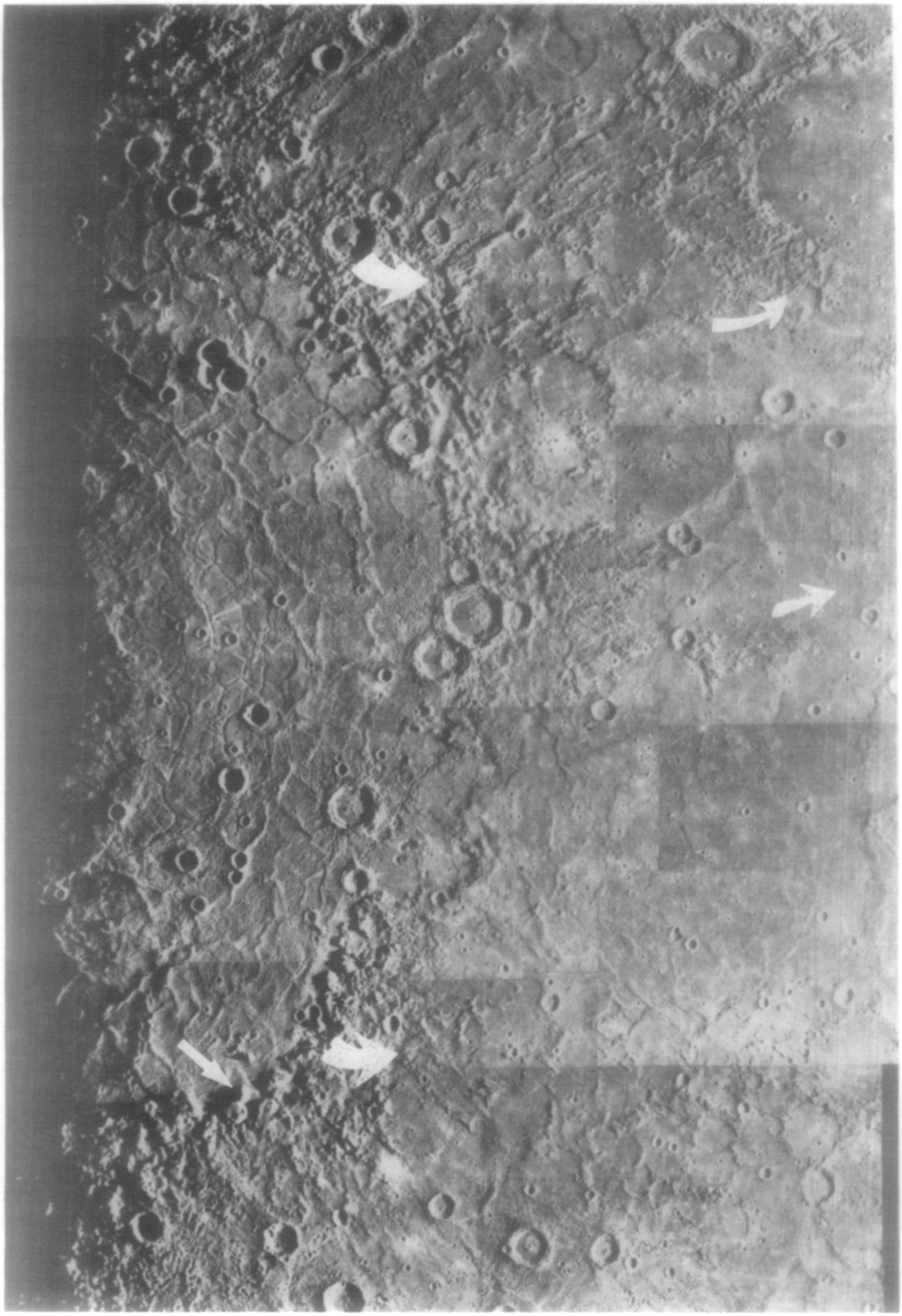

FIG. 4. The Caloris basin. The small straight arrow shows the type area of the Caloris Montes Formation that forms an almost continuous ring of blocky terrain surrounding the central basin. This blocky material is the morphologic counterpart of the materials of Montes Apenninus–Carpatus–Alpes at Imbrium and Montes Rook at Orientale. The large broad arrows show the outward transition zone

Wilhelms and McCauley (1971) called these blocky materials either pre-Imbrian rugged material or material of Montes Apenninus, both of which were interpreted as impact-deformed prebasin beckrock with or without a cover of late-arriving ejecta. Texturally, these two units are similar to the massif facies of the Montes Rook Formation around Orientale as mapped by Scott *et al.* (1977).

The distinctive knobby unit around the Imbrium basin was originally considered part of the Fra Mauro Formation by early workers, but was later defined as the Alpes Formation by Page (1970). It is also considered part of the Imbrium ejecta sequence, and generally lies beyond the blocky massifs that are at or near the basin rim. On the northeast side of the Imbrium basin near the craters Eudoxus and Aristoteles, the Alpes Formation extends as much as 400 km beyond Montes Caucasus. On the southwest it extends beyond Montes Carpatus a similar distance between the craters Kepler and Reinhold. The distribution of this unit around Imbrium is similar to but more extensive than the texturally similar Knobby Facies of the Montes Rook Formation around Orientale as mapped by Scott *et al.* (1977). The Fra Mauro Formation, as currently defined, is characterized by sinuous radially oriented ridges and troughs. It generally lies beyond both the Alpes Formation and the mountainous blocky massifs that surround the mare-filled central parts of Imbrium.

The location of the edge of the basin of excavation at Imbrium is an old problem. Wilhelms and McCauley (1971) connected the Montes Carpatus–Apenninus–Caucasus arc with the weak scarp that makes up the north shore of the Sinus Roris–Mare Frigoris trough. This placed lineated terrain, i.e., the Fra Mauro Formation, the massifs, and the blocky terrain of Montes Apenninus, on the same concentric arc at about the same distance from the center of the basin. At Orientale and Caloris, lineated terrain becomes prominent at a distance of about 100 to 150 km beyond the inner edge of the concentric zone that is occupied by massifs and knobby terrain. A better morphologic correlation at Imbrium is that the Caucasus and Alpes, despite their 200-km horizontal separation are parts of the same rim unit. Fielder (1965, pp. 106–108) recognized the similarities between the Alpes and Caucasus and postulated a large postbasin strike-slip fault to explain their offset. We interpret the observed displacement as an anomalously large rim tear fault formed during the cratering event. Features of this type have been descirbed in the walls of Meteor Crater by Shoemaker and Kieffer (1974) and in the rim of the Prairie Flat explosion crater by Roddy *et al.* (1977).

Much smaller lateral displacements are observed in parts of Montes Rook around Orientale (Fig. 2) and in Caloris Montes. We consider such structures to be indicative of the edge of the basin of excavation where impact-produced deformation is intense. Thus, each of the three basins is surrounded, except where buried by younger deposits, by an annulus of high, blocky materials that forms a distinctive and mappable stratigraphic unit. Outward from this unit, around all three basins, are irregular patches of knobby materials interspersed with swirly to lineated terrain.

The lineated terrain begins at the outer edge of the blocky unit and extends for 1000 kilometers or more. The prominence of the

between the Caloris Montes Formation and the lineated facies of the Van Eyck Formation. The type area of the lineated facies of the Van Eyck is shown by the long narrow curving arrow. The lineated facies of the Van Eyck spans the range of morphologies that characterize the inner and outer facies of the Hevelius Formation at Orientale and the Fra Mauro Formation and associated lineated materials at Imbrium. The type area for the Odin Formation is shown by the short eastward-pointing arrow. This unit closely resembles in texture and distribution the Alpes Formation around Imbrium (JPL special Mariner 10 mosaic). Image width is 1150 km.

rings or scarps, lying beyond the blocky and massif-dominated zones that surround the inner basins, varies dramatically. Orientale is surrounded on its eastern side by a well-developed outer scarp (Montes Cordillera) within which smooth surfaced, segmented massifs are absent. This scarp is extensively overlain by knobby or lineated ejecta indicating that it predates the final stages of the basin-forming event. Imbrium does not show a well-developed outer scarp; only a low and vague topographic high marks the beginning of the lineated terrain, the inner boundary of the Fra Mauro Formation. Caloris also has a poorly developed outer scarp. The development of ring structures thus varies with each of the basins, but comparable materials occur at roughly equivalent radial distances from the center of each. The spatial relations between the various types of bedrock and ejecta around each basin are likely a better key to the history of these basins then the poorly understood ring structures.

THE CALORIS GROUP

The formations that we now recognize within the Caloris Group from the rim of the basin outward are: (1) the Caloris Montes Formation (type area: the region around +18°, 184.5°, FDS-229), (2) the Nervo Formation (type area: the region near +40°, 177.5°, FDS-193), (3) the Odin Formation (type area: the region around +25°, 170°, FDS-72), (4a) the Van Eyck Formation, lineated facies (type area: the southwestern edge of the crater Van Eyck near +40°, 163°, FDS-189), and (4b) the secondary crater facies (type area: crater cluster at −7°, 166°, FDS-0529131). The type areas for these units, with the exception of the secondary crater facies of the Van Eyck Formation, are shown in Fig. 4. The units named here were delineated previously by Trask and Guest (1975) and by Guest and O'Donnell (1977). These units are portrayed more definitively on the 1:5,000,000-scale geologic maps of the Shakespeare (H-3) (Guest and Greeley, 1981) and Tolstoj (H-8) quadrangles (Schaber and McCauley, 1980).

The Caloris Montes Formation (Fig. 5) was informally called the Caloris mountains terrain by Trask and Guest (1975). It consists of a jumbled array of smooth-surfaced but highly segmented rectilinear mountain massifs that rise several kilometers above the surrounding terrain. Individual massifs are typically 30 to 50 km long; their surfaces are smooth to hackly. These massifs mark the crestline of the most prominent scarp or ring of the Caloris basin and grade outward into smaller blocks and lineated terrain. The massifs are separated by rectangular to irregular smooth-floored depressions; many of the depressions on the southeast side of the basin are gouge-like and resemble those in Montes Apenninus on the Moon. The Caloris Montes Formation is similar morphologically to the massif facies of the Montes Rook Formation around the Orientale basin (Scott *et al.*, 1977) and to materials of the Montes Carpatus–Apenninus–Caucasus–Alpes arc that surrounds the Imbrium basin. The Caloris Montes Formation, like the Montes Rook Formation, is interpreted as a basin rim deposit consisting of ejecta from deep within Caloris that is mixed with, but generally overlies, uplifted and highly fractured prebasin bedrock (McCauley, 1977). The inner edge of the unit, which is marked by basin-facing scarps, approximates the limit of the Caloris crater of excavation.

The Nervo Formation consists of rolling to locally hummocky plains that lie in intermassif depressions (Fig. 6). This unit was desribed as intermontane plains by Trask and Guest (1975) but not mapped separately. The plains generally lie within the annulus of rugged terrain of the Caloris Montes Formation and locally appear to drape and overlie some of the lower lying massifs. They are less smooth than the plains that surround and embay the exterior parts of Caloris and at most places lie at higher elevations. The Nervo Formation bears some resemblance to the patches of

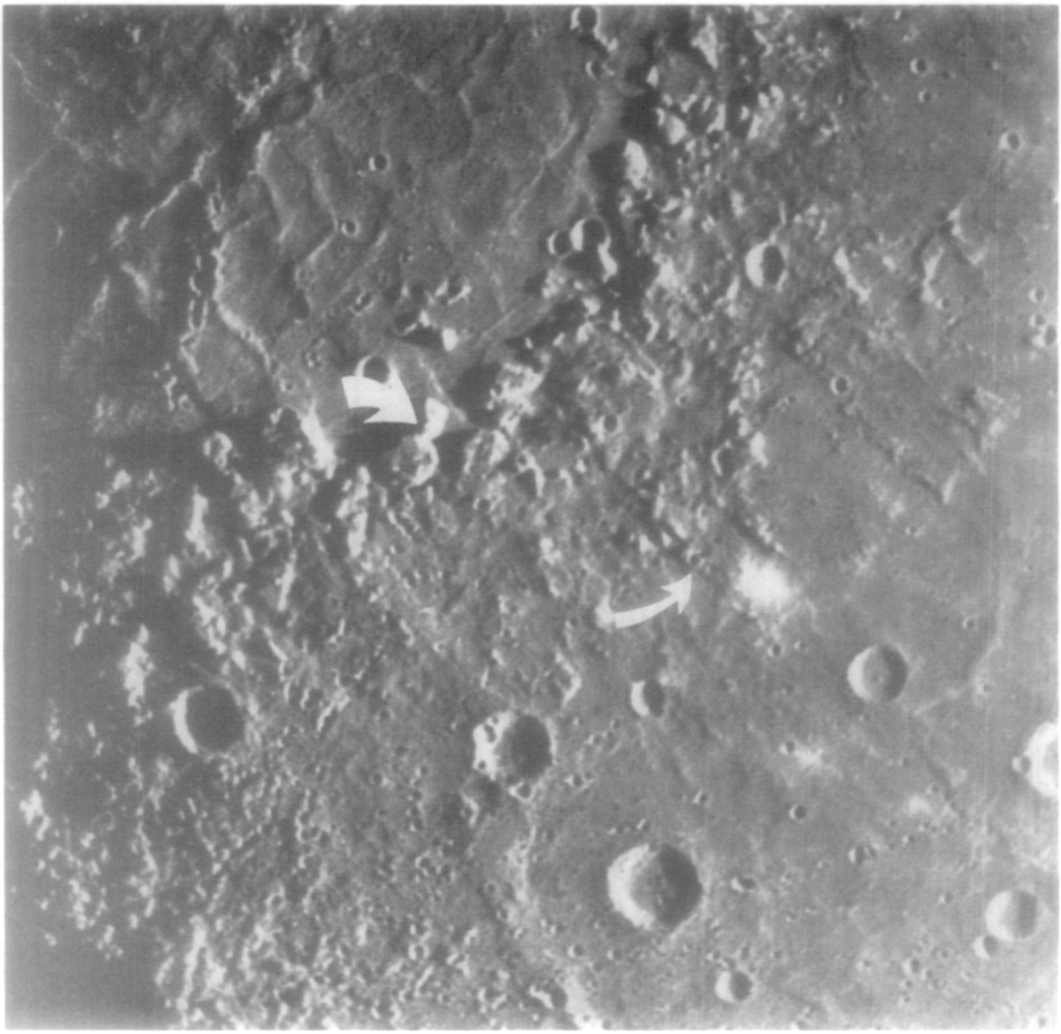

FIG. 5. Southeast side of Caloris basin. Large arrow indicates type area of the Caloris Montes Formation. Small curving arrow shows the lineated facies of the Van Eyck Formation; its closest recognized occurrence to the edge of the basin is about 150 km (FDS-229). Image width is 731 km.

smooth materials lying between the massifs in the circum-Imbrium region, particularly those of Montes Apenninus, some of which were mapped as terra materials undivided by Wilhelms and McCauley (1971). This unit has no counterpart in Orientale except for some very small, unmappable patches of intermassif plains. Most of the depressions between the massifs at Orientale are floored with the knobby facies of the Montes Rook Formation (Scott *et al.*, 1977). The Nervo Formation, or the intermontane plains as originally described by Trask and Guest (1975), was interpreted as fallback ejecta—an origin that seems consistent with its distribution pattern, relative roughness, and its perched position above the smoother plains that encompass the Caloris basin.

The Odin Formation was originally called the hummocky plains by Trask and Guest (1975) and described as closely spaced, smooth hills about 1 km across (Fig. 7). It occurs in extensive patches with diffuse outlines that lie as much as 600 to 800 km beyond Montes Caloris. The materials be-

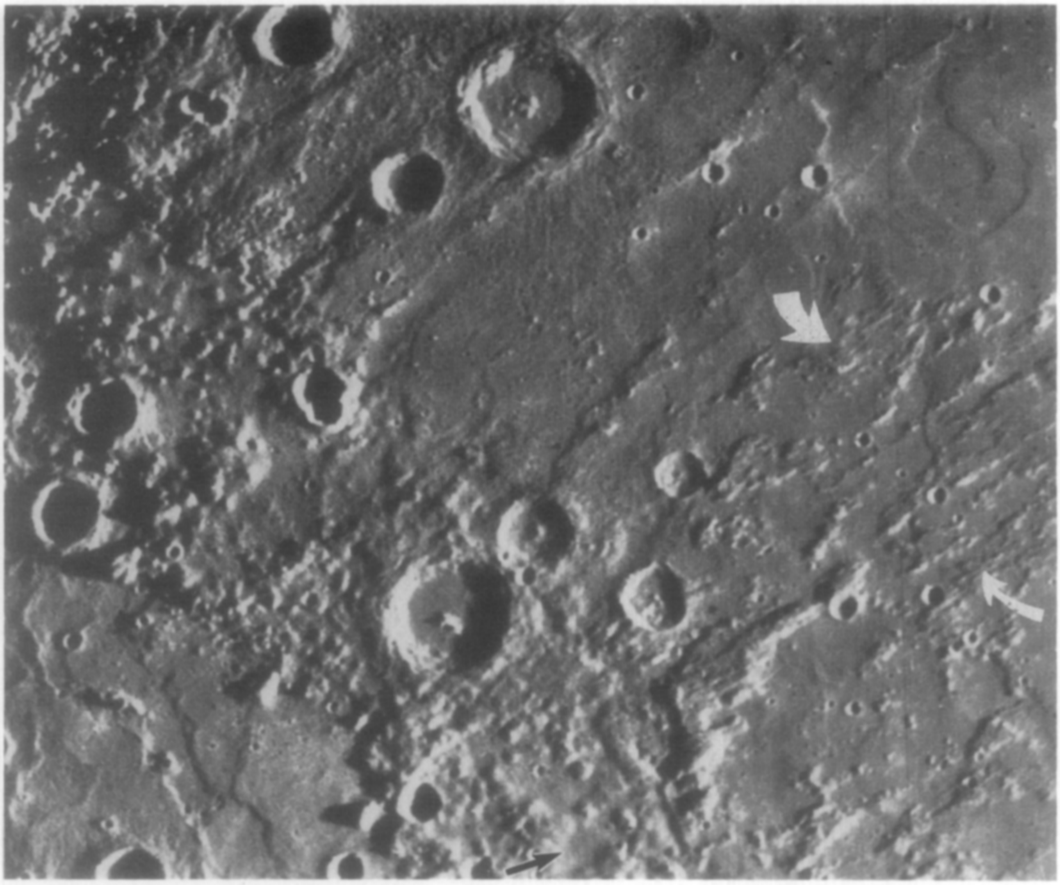

FIG. 6. Northeast side of Caloris basin. Small straight arrow at bottom of picture indicates type area of the Nervo Formation. This unit resembles the smooth plains that surround Caloris and embays the lineated facies of the Van Eyck but the Nervo is perched above the outer plains in intermontane troughs and locally appears to be draped over some of the massifs of the Caloris Montes Formation. A slightly swirly patch of the lineated facies of the Van Eyck is shown by the large arrow and a more typical radially lineated patch by the small curving arrow (FDS-193). Image width is 595 km.

tween individual closely spaced hills consist of smooth plains identical to those that surround and embay most of Caloris. The distribution of the Odin is highly dependent on resolution and lighting but it appears similar to that of the Alpes Formation on the Moon. The Odin, like the Alpes, occurs in broad lobes beyond the main basin scarp such as the one seen in Odin Planitia. The Odin also resembles the knobby facies of the Montes Rook that lies on top of and beyond the massif facies in and around the Orientale basin. The Odin Formation is interpreted as part of the Caloris ejecta sequence, but its mode of origin is less clear than for the other formations in the Caloris Group. It probably consists of blocky, high-angle, late-arriving ejecta from deep within the Caloris cavity that was later partly buried by smooth plains.

The Van Eyck Formation is the most distinctive of the circum-Caloris stratigraphic units and is here divided into two facies, the lineated and the secondary-crater facies. Like the other formations in the Caloris Group, it also was first recognized by Trask and Guest (1975) and called Caloris lineated terrain. The inner boundary of the lineated facies is generally coincident with the weak, outer Caloris scarp. This

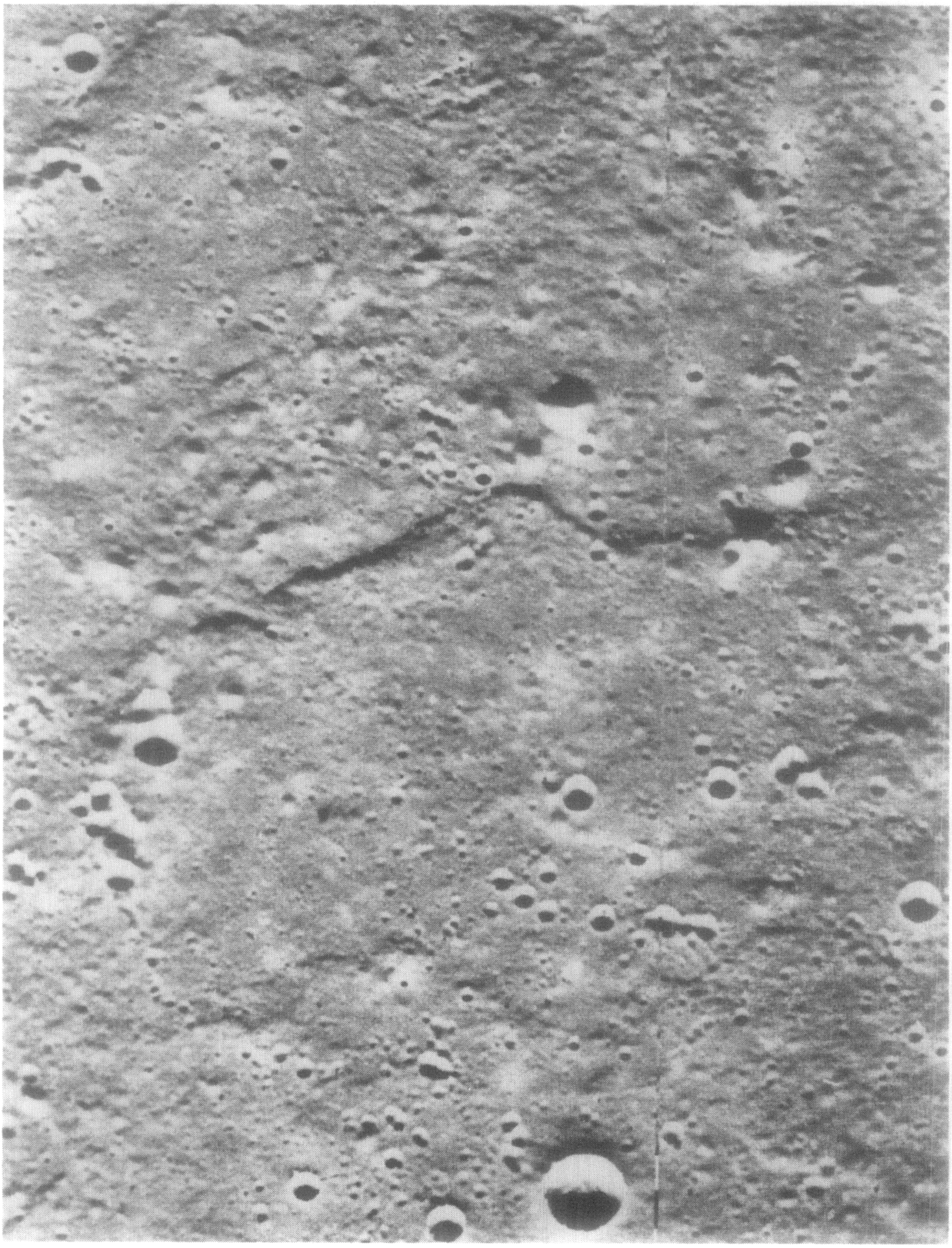

FIG. 7. Type area of the Odin Formation about 500 km east of the edge of the Caloris basin. The outer boundaries of this unit are difficult to define and the terrain between individual kilometer-scale knobs consists of smooth plains as is the case for the Alpes Formation and the knobby facies of the Montes Rook Formation (FDS-72). Image width is 291 km.

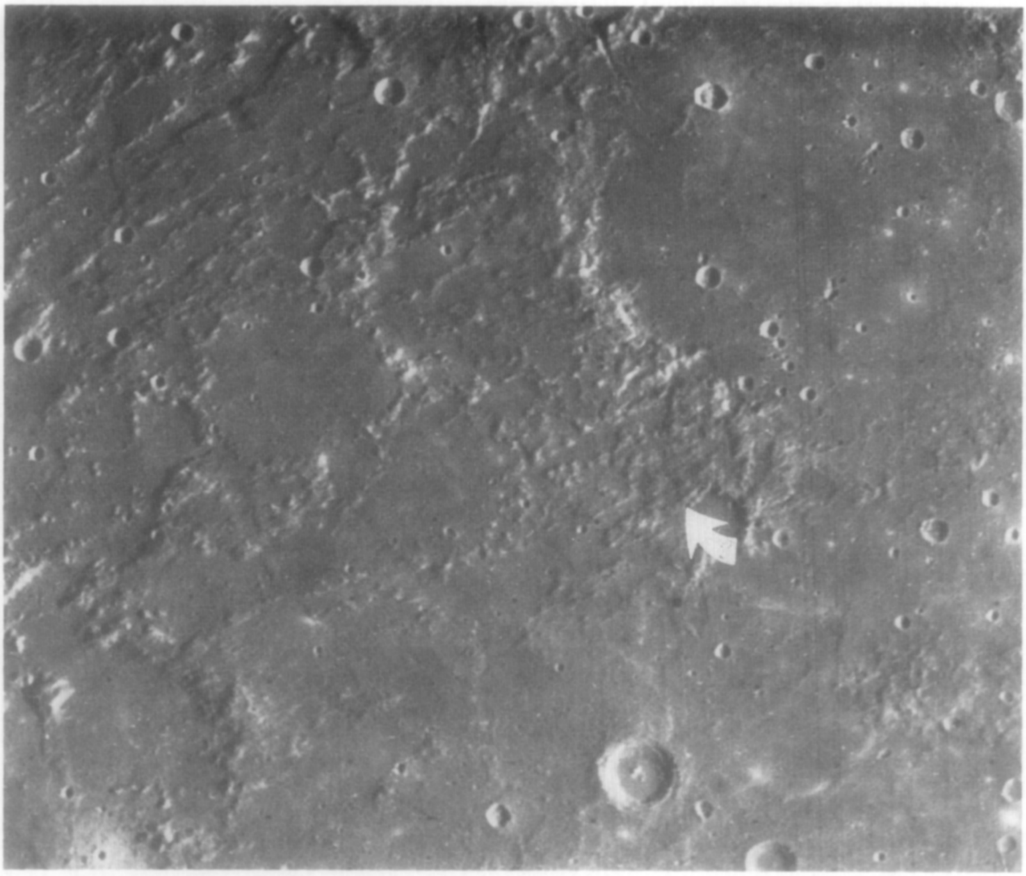

FIG. 8. Type area (arrow) of the lineated facies of the Van Eyck Formation on the southeast flank of the large double ring crater of the same name. This ejecta unit like the others of the Caloris Group is extensively embayed by smooth plains material (FDS-189). Image width is 584 km.

unit is made up of radial ridges and grooves and locally swirly terrain that is extensively embayed by smooth plains (Figs. 5, 6, 8). The lineated facies of the Van Eyck Formation is similar in appearance to the Fra Mauro Formation around the Imbrium basin but considerably more degraded and more extensively embayed by smooth plains. The swirly ridges and elongate depressions are less abundant than they are in the Fra Mauro and the much fresher inner facies of the Hevelius Formation around Orientale. Unlike the Hevelius, the lineated facies of the Van Eyck cannot be divided into an inner and outer facies on the basis of texture and subdual of pre-basin topography. In general, the Van Eyck even close to the weak outer Caloris scarp looks like the distal ends of the Fra Mauro and also what was mapped as lineated material around Imbrium by Wilhelms and McCauley (1971). The lineated facies of the Van Eyck is interpreted as ballistically emplaced ejecta mixed with prebasin bedrock. The close-in distribution of this facies of the Van Eyck is consistent with the gravitational effects on cratering postulated by Gault *et al.* (1975). It is difficult to define individual secondary craters within the Van Eyck, but many of the plains-filled depressions between radial ridges were undoubtedly formed by secondary cratering. At a distance of about one basin diameter, numerous individual clusters and chains of moderately well preserved craters become more apparent as the ejecta blanket be-

FIG. 9. Type area of the secondary crater facies of the Van Eyck Formation. These clusters and chains of 5- to 20-km craters, all in about the same state of preservation, appear very similar to the secondary craters identified around Imbrium and Orientale (FDS-0529131). Image width is 176 km.

comes more dispersed. These craters are interpreted as Caloris secondaries formed by far-flung ejecta (Fig. 9). These have been included as a separate facies of the Van Eyck Formation because of their stratigraphic significance in dating other basins, craters, and plains.

The plains within the floor of the central part of Caloris are a special problem and are therefore not included in the Caloris Group. These plains have some features in common with the Maunder Formation in the floor of Orientale (McCauley, 1977; Scott *et al.*, 1977). However, they do not show the radial and circumferential ridges characteristic of the Maunder which led to its interpretation as a basin floor unit, and they have a more open and coarser fracture pattern than does the Maunder Formation. In addition, the Caloris ridges and the fractures that cut them have a crude rhombic pattern that led Strom *et al.* (1975) to conclude that the floor of the basin subsided and then was gently uplifted to produce the open tension fractures observed. The ridges in the floor of Caloris lack the crenulated crests that are common on lunar ridges. Regardless of the origin and tectonic history of these plains, they clearly represent a deep-fill unit that now obscures the floor of the Caloris basin.

RELATION OF THE MERCURY CRATER DEGRADATION SEQUENCE TO THE CALORIS EVENT

Beyond the recognizable geologic imprint of the Caloris event on the surface of Mercury, the state of preservation of craters in the size ranges 30 to 100 km and above 100 km was proved helpful for relative age dating. Techniques for using the morphology of large craters as a dating tool were established for the Moon by Pohn and Offield (1970). The method depends on the degree of degradation of certain morphologic components of craters assuming that each impact crater in a given size range had approximately the same initial form. Thus craters of similar size that show similar states of preservation are considered to be of about the same age. The morphologic components used are rays, secondary craters, various ejecta facies, rim sharpness, inner terraces and central peaks. With in-

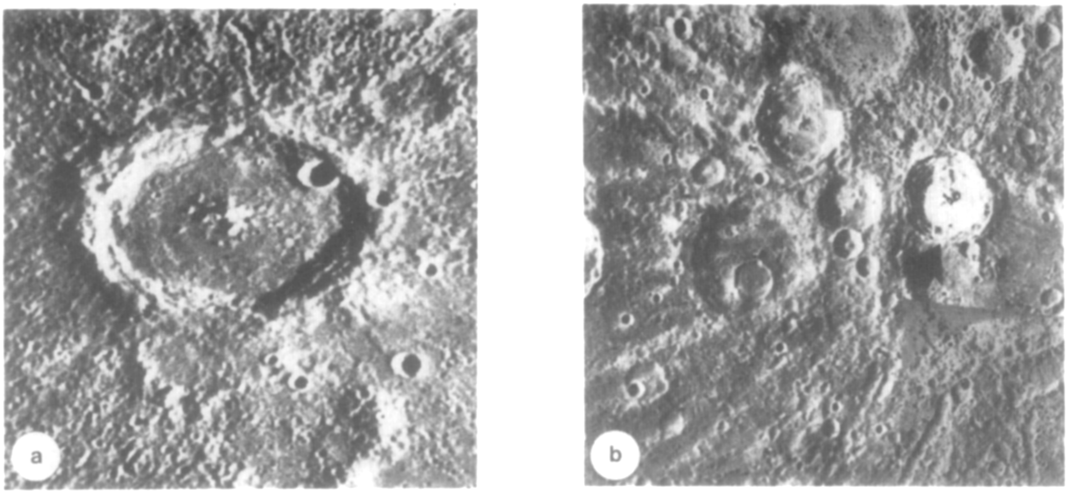

(a) Example of c_5, Verdi (65°N., 168°), 150-km diameter (FDS 166): flat, hummocky floor with multiple central peak; wall extensively terraced; rim circular; radial ejecta blanket close-in; well-defined, continuous field of crisp satellite craters.

(b) Example of c_5, Kruiper (11°S., 32°), 60-km diameter (FDS 27304): sharp-appearing, greater depth–diameter ratio than larger c_5 craters; flat floor with central peak; wall extensively terraced; sharp contact between wall and floor; secondary crater field identifiable with photographs of adequate resolution; rayed craters included, but all rays cannot be distinguished at low sun angles; dark halos may also be present on the rim.

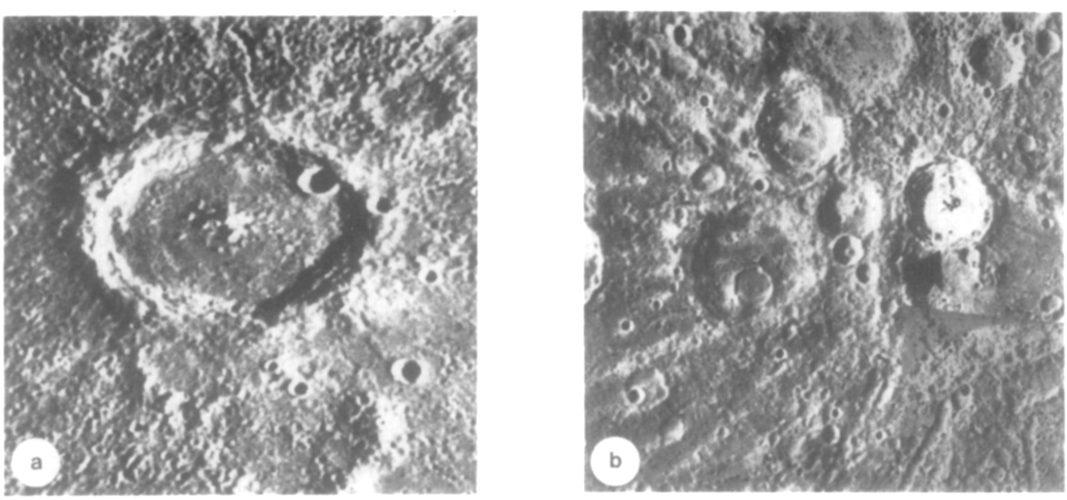

(c) Example of c_4, Strindberg (53°N., 135°) 165-km diameter (FDS 150): flat floor, central peak or ring common; filled or partially filled with plains material; wall terraced, terraces disrupted by slumping; rim scalloped; radial ejecta blanket close-in; well-preserved, extensive, field of satellite craters.

(d) Example of c_4, Amru Al-Qays (13°N., 176°), 50-km diameter (FDS 226: not as sharp appearing as c_5; flat floor; terraces present but subdued and interrupted; central peak present; contact at base of wall with floor sharp; indications of satellitic field on photographs of high resolution and low to moderate sun angle.

FIG. 10. An interpretation scheme for relative age determination of Mercurian craters (N. J. Trask).

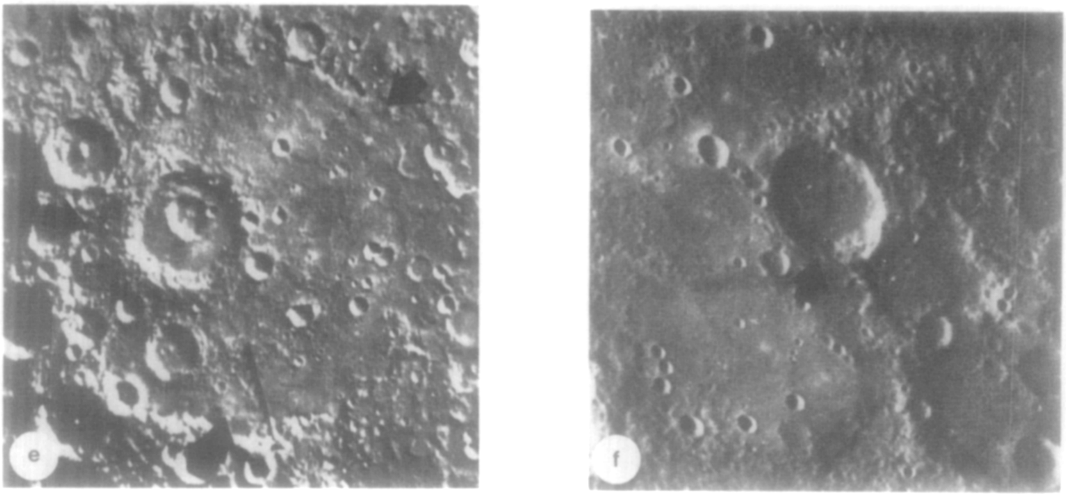

(e) Example of c_3, Dostoevskij (45°S., 177°), 390-km diameter (FDS 166844): flat floor, some with central peak or ring; filled or partially filled with plains material; vague terraces in some smaller basins and craters; rim irregular but continuous; some evidence of radial ejecta blanket; some chains and clusters of satellitic craters but not a continuous field.

(f) Example of c_3, unnamed crater (45°S., 32°), 60-km diameter (FDS 27286): rim rounded; terraces in some larger examples, radial channels on wall of some examples; flat floor, filled with plains material; floor–wall boundary indistinct; central peak rare; no visible satellitic craters.

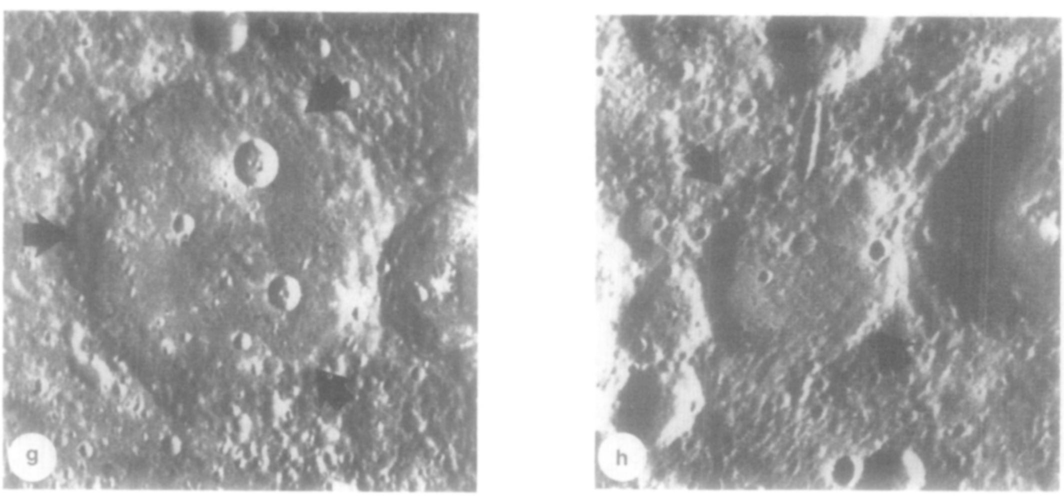

(g) Example of c_2, Sei (63°S., 88°), 130-km diameter (FDS 166675): flat floor, central peaks and rings rare; filled or partially filled with plains material; weakly developed terraces in some examples; rim low, continuous; covered with superposed primary and secondary craters; no recognizable field of satellitic craters connected with crater or basin.

(h) Example of c_2, unnamed crater (1°N., 18°), 55-km diameter (FDS 27438): shallow pan-shaped craters, rim rising only slightly above crater floor; flat floor filled with plains material; some central peaks; no satellitic craters.

FIG. 10—*Continued.*

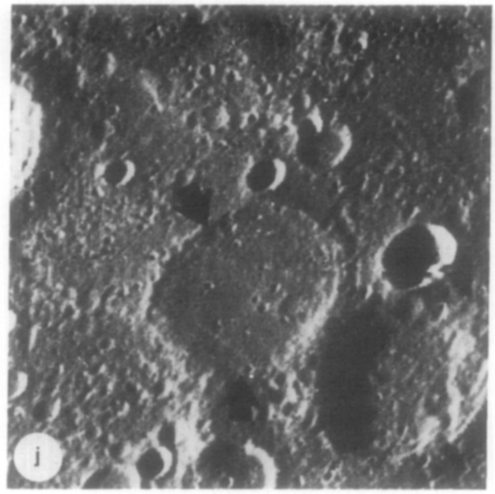

(i) Example of c_1, Imhotep (18°S., 38°), 160-km diameter (FDS 27367): flat floor with no central peak or ring; filled with plains material; no terraces; low, discontinuous rim rising only slightly above adjacent plains; no satellitic craters.

(j) Example of c_1, unnamed crater (6°N., 17°), 70-km diameter (FDS 27443): rim almost obliterated; no central peak; plains material covers floor; no secondary crater field.

FIG. 10—*Continued.*

creasing age and greater density of smaller superposed craters, these components become more subdued or are totally obliterated. The end product of impact aging is generally a vague, incompletely cratered but smooth-crested circular ridge. Postimpact volcanic activity may bury or destroy certain crater components such as ejecta facies or secondary craters, but other components such as the rim and terraces may be preserved so that the crater can still be dated. A somewhat younger, larger crater or one of nearly equivalent size forming near a slightly older one will produce proximity aging and make the earlier crater appear older than it actually is. With younger craters this phenomenon can be recognized and age corrections applied, but it remains a problem for the older large craters that are generally more closely packed.

Newell Trask (personnal communication, 1976) in a written memorandum to Mercury geologic mappers proposed and illustrated a crater morphology dating scheme that has received general acceptance. Despite the stronger gravitational field of Mercury that reduces the dispersion of ejecta and secondaries, relative crater ages can be established with fair precision, though not quite as well as on the Moon. Figure 10 is a recent modification of the original classification proposed by Trask. Although useful over wide areas of the Mariner 10 coverage, the degradation sequence is not sensitive enough for detailed stratigraphic classifications. However, if tied to an established marker horizon such as the Caloris Group, the crater aging sequence becomes a more powerful tool that can be used to establish a pre- and post-Caloris chronology for much of Mercury (Schaber and McCauley, 1980).

Numerous craters in the 30- to 100-km size range are clearly superposed on the Caloris ejecta assemblage. Most of these are of the c_4 and c_5 (youngest craters have the highest subscript numbers) type such as Nervo and March. A few smaller craters—mostly 30 to 50 km in size, designated as upper c_3—are also superposed on the Caloris Group. These include the unnamed craters near +10°, 170°; +14°, 179°; +1°, 182°; and

+43.5°, 176° (Fig. 4). Thus the Caloris event appears to have occurred in late c_3 time.

The formal rock-stratigraphy presented here provides a useful shorthand for discussions of the stratigraphy of Mercury. It should help to prevent the type of descriptive confusion that crept into the literature of the Orientale basin on the Moon. If other basins and craters can be tied into the Caloris basin over the rest of Mercury using data from Mariner 10 and any later orbiter mission, this stratigraphy may later be useful in helping to establish a time stratigraphy consisting of formal systems and periods in the history of Mercury.

REFERENCES

COHEE, G. V. (1974). Stratigraphic nomenclature. In *Reports of the U.S. Geological Survey*. U.S. Geological Survey, Flagstaff, Ariz.

DAVIES, M. E., DWORNIK, S. E., GAULT, D. E., AND STROM, R. G. (1978). *Atlas of Mercury*. NASA Spec. Publ. SP-423.

FIELDER, G. (1965). *Lunar Geology*. Dufour Editions, Chester Springs, Pa.

GAULT, D. E., GUEST, J. E., MURRAY, J. B., DZURISIN, D., AND MALIN, M. C. (1975). Some comparisons of impact craters on Mercury and the Moon. *J. Geophys. Res.* **80**, 2444–2460.

GAULT, D. E., QUAIDE, W. L., AND OBERBECK, V. R. (1968). Impact cratering mechanics. In *Shock Metamorphism of Natural Materials* (B. M. French and N. M. Short, Eds.), pp. 89–99. Mono, Baltimore.

GUEST, J. E., AND GREELEY, J. E. (1981) *Geologic Map of the Shakespheare Quadrangle of Mercury*. U.S. Geological Survey Misc. Geol. Inv. Series I. In press.

GUEST, J. E., AND O'DONNELL, W. P. (1977). Surface history of Mercury: A review. *Vistas in Astron.* **20**, 273–300.

HACKMAN, R. J. (1966). *Geologic Map of the Montes Apenninus Region of the Moon*. U.S. Geological Survey Misc. Inv. Series I-463.

HEAD, J. W. (1974). Orientale multi-ring basin interior and implications for the petrogenesis of lunar highland samples. *The Moon* **11**, 327–356.

HODGES, C. A., AND WILHELMS, D. E. (1976). Formation of lunar basin rings. In *Proceedings, 25th International Geol. Cong. Sydney*, **2**, pp. 612–613.

MCCAULEY, J. F. (1967). *Geologic Map of the Hevelius Region of the Moon*. U.S. Geological Survey Misc. Inv. Series I-491.

MCCAULEY, J. F. (1977). Orientale and Caloris. *Phys. Earth Planet. Interiors* **15**, 220–250.

MOORE, H. J., HODGES, C. A., AND SCOTT, D. H. (1974). Multi-ring basins illustrated by Orientale and associated features. *Geochim. Cosmochim. Acta* **1**, Suppl. 5, 71–100.

MORRISON, R. H., AND OBERBECK, V. R. (1975). Geomorphology of crater and basin deposits—Emplacement of the Fra Mauro Formation. *Geochim. Cosmochim. Acta* **3**, Suppl. 6, 2503–2530.

OBERBECK, V. R. (1975). The role of ballistic erosion and sedimentation in lunar stratigraphy. *Rev. Geophys. Space Phys.* **13**, 337–362.

PAGE, N. J. (1970). *Geologic Map of the Cassini Quadrangle of the Moon*. U.S. Geological Survey Misc. Geol. Inv. Series I-666.

POHN, H. A., AND OFFIELD, T. W. (1970). Lunar crater morphology and relative age determination of lunar geologic units. Part I. Classfication, In *Geological Survey Research 1970*. U.S. Geological Survey Prof. Paper 700-C, pp. C153–C162.

RODDY, D. J. (1976). High-explosive cratering analogs for bowl-shaped central uplift, and multi-ring impact craters. *Geochim. Cosmochim. Acta* **3**, Suppl. 7, 3027–3056.

RODDY, D. J., ULRICH, G. W., SAUER, F. M., AND JONES, G. H. S. (1977). Cratering motions and structural deformation in the rim of the Prairie Flat multi-ring explosion crater. *Geochim. Cosmochim. Acta*, Suppl. 8, 3389–3407.

SCHABER, G. G., AND MCCAULEY, J. F. (1980). *Geologic Map of the Tolstoj Quadrangle of Mercury*. U.S. Geol. Survey Misc. Geol. Inv. Series I-1199.

SCOTT, D. H., MCCAULEY, J. F., AND WEST, M. N. (1977). *Geologic Map of the West Side of the Moon*. U.S. Geological Survey Misc. Geol. Inv. Series I-1034.

SCOTT, D. H., AND CARR, H. M. (1978). *Geologic Map of Mars*. U.S. Geological Survey Misc. Geol. Inv. Series I-1081.

SHOEMAKER, E. M. (1962). Interpretation of lunar craters. In *Physics Astronomy of the Moon* (Z. Kopal, Ed.), pp. 283–359. Academic Press, London/New York.

SHOEMAKER, E. M. (1963). Impact mechanics at Meteor Crater, Arizona. In *The Solar System* (G. P. Kuiper, Ed.), Vol. 4, pp. 301–336. Univ. of Chicago Press, Chicago.

SHOEMAKER, E. M., AND HACKMAN, R. J. (1962). Stratigraphic basis for a lunar time scale. In *The Moon—IAU Symposium 14, Leningrad, 1960*, pp. 289–300. Academic Press, London/New York.

SHOEMAKER, E. M., AND KIEFFER, S. W. (1974). Guidebook to the Geology of Meteor Crater, Arizona. In *34th Annual Meeting of the Meteoritical Society, August 4, 1974*.

STROM, R. G., TRASK, N. J., AND GUEST, J. E. (1975). Tectonism and volcanism on Mercury. *J. Geophys. Res.* **80**, 2478–2507.

STROM, R. G. (1979). Mercury: A Post-mariner 10 Assessment. *Space Sci. Rev.* **24**, 3–70.

STUART-ALEXANDER, D. E., AND WILHELMS, D. E. (1975). The Nectarian System, a new lunar time-stratigraphic unit. In *Geological Survey Research, 1975*, Vol. 3, pp. 53–58. U.S. Geological Survey.

TRASK, N. J., AND GUEST, J. E. (1975). Preliminary geologic terrain map of Mercury. *J. Geophys. Res.* **80**, 2461–2477.

WILHELMS, D. E. (1976). Mercurian volcanism questioned. *Icarus* **28**, 551–558.

WILHELMS, D. E. AND MCCAULEY, J. F. (1971). *Geologic Map of the Near Side of the Moon.* U.S. Geological Survey Misc. Geol. Inv. Series I-703.

WILHELMS, D. E., HODGES, C. A., AND PIKE, R. J. (1977). Nested-crater model of lunar ringed basins. In *Impact and Explosion Cratering: Planetary and Terrestrial Applications* (D. J. Roddy, R. O. Pepin, and R. B. Merrill, Eds.), pp. 539–562. Pergamon, New York.